

ON THE USE OF DESIGN-BASED SIMULATIONS *

Bruno Ferman[†]

Abstract

Design-based simulations—procedures that hold realized outcomes fixed and generate variation by resampling treatment assignment or shocks—are widely used in both methodological and applied work to assess inference procedures. This paper studies the extent to which such simulations are informative about inference validity. Focusing on shift-share designs, we show that standard simulations that fix outcomes and resample shocks may rely on a data-generating process that is not aligned with the true one. In particular, these simulations confound true treatment effects with error dependence, potentially overstating inference distortions due to spatial correlation. We propose alternative simulation designs that circumvent this problem and illustrate their use in prominent empirical applications. Our results highlight that the usefulness of design-based simulations depends critically on how closely the simulated data-generating process aligns with the true one.

Keywords: design-based simulations, inference, shift-share designs, spatial correlation

JEL Codes: C12; C21

*I gratefully acknowledge financial support from FAPESP and CNPq. An earlier version of part of this material was presented in Ferman (2019).

[†]email: bruno.ferman@fgv.br; Sao Paulo School of Economics – FGV

1 Introduction

Simulation-based analyses play a central role in econometric research. They are routinely used to study the finite-sample properties of estimators and inference procedures, and to illustrate potential failures of commonly used methods. An important class of such exercises consists of what we refer to as *design-based simulations*, in which realized outcomes are treated as fixed and uncertainty in the simulations is generated by resampling treatment assignment, shocks, or other components of the research design.

Design-based simulations have been used in methodological papers to illustrate inference problems in prominent empirical settings. For example, Bertrand et al. (2004) simulate placebo laws using state-level data on female wages from the Current Population Survey to illustrate severe size distortions of conventional inference methods in difference-in-differences (DiD) designs caused by serial correlation. More recently, design-based simulations have played a central role in the analysis of inference methods in shift-share designs. Adão et al. (2019) and Borusyak et al. (2021) use simulations based on resampling sectoral shocks to illustrate how spatial correlation can invalidate standard inference procedures and to analyze the properties of alternative inference methods in this setting. Related simulation-based approaches are also considered by de Chaisemartin and Ramirez-Cuellar (2024) in the context of small-strata randomized experiments. Beyond their use as illustrative tools in methodological work, design-based simulations can also be employed by applied researchers as application-specific diagnostics. In this context, researchers may use design-based simulations tailored to their empirical design to assess whether a given inference method is likely to perform well in their specific setting.

In design-based simulations, researchers usually define a data-generating process (DGP) based on an empirical application or a specific dataset, in which potential outcomes are held fixed and the null hypothesis is satisfied by construction. Interpreting the results from such simulations, however, can be subtle. Whether the resulting rejection frequencies are

informative about validity of an inference method in the original empirical setting depends critically on how the DGP used in the design-based simulations relates to the true DGP along dimensions relevant for inference. As a result, design-based simulations may be highly informative in some settings, but potentially misleading in others. Moreover, design-based simulations have often been used to illustrate issues related to the distribution of the errors (for example, serial or spatial correlation), which at first glance appears at odds with the fact that potential outcomes—and therefore errors—are held fixed in these simulations.

This paper studies the properties of design-based simulations, with a particular focus on shift-share designs, where such simulations have been especially influential in recent methodological debates. We show that when treatment effects are present, standard design-based simulations may mechanically confound treatment effects with error dependence, overstating the over-rejection of inference methods that do not allow for spatial correlation. We then discuss two alternative design-based simulation designs that circumvent these problems. Our analysis also clarifies how design-based simulations, despite holding errors fixed, can nonetheless be informative about characteristics of the error distribution. We also show that the alternative design-based simulations we propose can be more informative about distortions due to spatial correlation than tests based on the statistical significance of regressions using pre-treatment outcomes.

Finally, we analyze the use of design-based simulations in three shift-share design empirical applications. Our results reinforce the central insight of Adão et al. (2019) that standard inference methods should be used with caution in shift-share applications, given the possibility of spatial correlation. At the same time, we show that commonly used design-based simulations tend to overstate the magnitude of size distortions attributable to spatial correlation, because they confound true treatment effects with error dependence. As a result, applied researchers who rely on standard design-based simulations in their own empirical applications may be led to misleading conclusions about the relative performance of alternative inference methods. We illustrate how the alternative simulation

designs we propose avoid these issues and provide more informative guidance for inference in shift-share designs.

2 Design-based simulations in randomized experiments

We consider first a simple setting of randomized experiments, in which we can illustrate the fundamental problem that generally prevents design-based simulations from recovering the true DGP in an empirical application, even when the distribution of treatment allocation is known.

Suppose we observe $i = 1, \dots, N$ individuals whose potential outcomes are given by $Y_i(0)$ and $Y_i(1)$, and the only source of uncertainty comes from the treatment allocation $\mathbf{T} = (T_1, \dots, T_N)$, which is assumed to have a known distribution (Abadie et al., 2020, 2022; Fisher, 1935; Neyman, 1990). The target parameter is the sample average treatment effect (SATE), $\frac{1}{N} \sum_{i=1}^N (Y_i(1) - Y_i(0))$.¹ In this case, inference using robust standard errors is asymptotically valid for the SATE in this sampling framework when $N \rightarrow \infty$ (although in some cases it may be conservative). Still, it might be that an econometrician or an applied researcher wants to study the properties of such inference method in a specific empirical application with a fixed N .

In this setting, the true DGP is characterized by $\{Y_i(0), Y_i(1)\}_{i=1}^N$ and the distribution of \mathbf{T} . Therefore, if we knew $Y_i(0)$ and $Y_i(1)$ for all i , then knowledge of the distribution of \mathbf{T} would provide all information needed to recover the true probability of rejection for a test based on, for example, robust standard errors. More specifically, note that the distribution of the t-statistic with robust standard errors will be a function of $\{Y_i(0), Y_i(1)\}_{i=1}^N$ and \mathbf{T} , where the only stochastic component in this design-based setting is \mathbf{T} . Therefore, we would be able to calculate the exact probability that the t-statistic would be greater than a given

¹Abadie et al. (2020) and Abadie et al. (2022) also consider the possibility of sampling uncertainty. In this case, an alternative target parameter would be the population average treatment effect. For simplicity, we abstract from that.

critical value and, thus, the probability of rejection.²

However, we do not know $Y_i(0)$ and $Y_i(1)$ for all i . In this case, a commonly used way to construct design-based simulations in this setting is to hold the vector of realized outcomes fixed (\mathbf{Y}), and consider different allocations of \mathbf{T} coming from the known distribution of \mathbf{T} . Then, for each allocation of \mathbf{T} we estimate the parameter of interest and test the null using the inference method being analyzed. This design-based simulation implicitly considers a DGP in which potential outcomes are given by $\{\tilde{Y}_i(0), \tilde{Y}_i(1)\}_{i=1}^N$, where $\tilde{Y}_i(1) = \tilde{Y}_i(0) = Y_i$, and the true distribution of \mathbf{T} . Therefore, in this DGP the null hypothesis that the SATE equals zero is true, because $\frac{1}{N} \sum_{i=1}^N (\tilde{Y}_i(1) - \tilde{Y}_i(0)) = 0$, and the design-based simulations gives us the size of this test if potential outcomes were given by $\{\tilde{Y}_i(0), \tilde{Y}_i(1)\}_{i=1}^N$.

The fundamental challenge with this approach is that the true DGP would not be given by $\{\tilde{Y}_i(0), \tilde{Y}_i(1)\}_{i=1}^N$ if $Y_i(1) \neq Y_i(0)$ for some i . Hence, even if we know the distribution of \mathbf{T} , a design-based simulation holding \mathbf{Y} fixed would not necessarily recover the true finite-sample rejection rate of a given inference method or the true coverage for a confidence interval. It is therefore crucial to understand how the DGP underlying such design-based simulations may differ from the true DGP along dimensions that are relevant for finite-sample rejection rates of the inference method under consideration. For example, suppose that $\{Y_i(0)\}_{i=1}^N$ and $\{Y_i(1)\}_{i=1}^N$ are symmetric and single-peaked in their empirical distribution, with $Y_i(1) = Y_i(0) + \beta$ for all i and some constant $\beta > 0$. In this case, a design-based simulation that fixes \mathbf{Y} and sets $\tilde{Y}_i(1) = \tilde{Y}_i(0) = Y_i$ would instead consider a DGP in which the distributions $\{\tilde{Y}_i(0)\}_{i=1}^N$ and $\{\tilde{Y}_i(1)\}_{i=1}^N$ may be dual peaked, thus differing fundamentally from the true DGP.

In Section 3, we analyze in detail how the fact that design-based simulations do not recover exactly the true DGP implies an important challenge for the use of design-based simulations in shift-share designs.

²Since the true SATE may differ from zero, calculating the size of the test in this hypothetical scenario would require testing the null $H_0 : SATE = \frac{1}{N} \sum_{i=1}^N (Y_i(1) - Y_i(0))$, that is, the true SATE. Of course, since $\frac{1}{N} \sum_{i=1}^N (Y_i(1) - Y_i(0))$ is generally unknown, this is not feasible in practice.

Remark 1. *While similar at first glance, this type of design-based simulation is conceptually distinct from randomization inference in randomized experiments. In randomization inference, permutations of the treatment assignment are used to conduct exact finite-sample tests of a sharp null hypothesis, such as $Y_i(1) = Y_i(0)$ for all i . In contrast, the design-based simulation described above uses permutations of the assignment to construct a DGP based on the observed outcomes in the application at hand, with the goal of evaluating the finite-sample properties of an alternative inference procedure (e.g., a t -test with robust standard errors for hypotheses regarding the SATE).*

3 Design-based simulations in shift-share designs

3.1 Shift-share design framework

We consider now the use of design-based simulations in shift-share design settings. Shift-share designs are specifications that study the impact of a set of shocks on units differentially exposed to them. Consider a setting with $i = 1, \dots, N$ regions that are subject to $f = 1, \dots, F$ aggregate shocks \mathcal{X}_f . The shift-share variable is given by $x_i = \sum_{f=1}^F w_{if} \mathcal{X}_f$, where the shares w_{if} reflect how shock \mathcal{X}_f affects unit i . The regression model is then given by

$$y_i = \beta_0 + \beta x_i + \epsilon_i, \tag{1}$$

where β reflects the effect of x_i on y_i . Let \mathbf{y} be the $N \times 1$ vector of outcomes, and Ω be the $N \times F$ matrix with all shares for all regions.

A key insight from Adão et al. (2019) is that, when testing the null $H_0 : \beta = 0$, an important challenge in this setting is that the error term ϵ_i may be spatially correlated. In particular, if regions with similar shares tend to have correlated errors, this spatial correlation leads to over-rejection if one relies on robust or cluster-robust standard errors.

In order to illustrate this issue, Adão et al. (2019) consider design-based simulations in which they hold \mathbf{y} and Ω fixed, and draw realizations of $\{\tilde{\mathcal{X}}_f\}_{f=1}^F$ for a given distribution for the shocks. For each realization of the shocks in these simulations, they estimate the shift-share estimator from $y_i = \gamma_0 + \gamma \tilde{x}_i^b + \tilde{\epsilon}_i$, where $\tilde{x}_i^b = \sum_{f=1}^F w_{if} \tilde{\mathcal{X}}_f^b$, and test the null $\gamma = 0$ using robust or cluster-robust standard errors. In these simulations, they find rejection rates much higher than the nominal size of the tests.

Adão et al. (2019) and Borusyak et al. (2021) propose interesting alternatives for inference taking into account the possibility of spatial correlation. They consider a design-based setting, where shocks \mathcal{X}_f are stochastic, while potential outcomes and shares are conditioned on.³ A simplified version of their potential outcomes model is given by $y_i(x) = y_i(0) + \beta x$, where we assume for simplicity linearity and treatment effect homogeneity across shocks. In this setting, the identification assumption is that $\mathbb{E}[\mathcal{X}_f | \mathcal{L}] = c$ for a constant c , where \mathcal{L} includes potential outcomes and shares. The inference methods they developed are asymptotically valid in this sampling framework when (i) shocks are independent, (ii) the number of shocks goes to infinity, and (iii) the size of each shock becomes asymptotically negligible.⁴ The fact that they developed their theory in this framework does not necessarily mean that the focus in shift-share designs should be on inference conditional on \mathcal{L} . As discussed by Adão et al. (2019), the idea of conditioning on potential outcomes is so that they “can allow for any correlation structure of the regression residuals across regions.”

3.2 Design-based simulations in shift-share designs: theory

Consider now the shift-share design setting from Section 3.1. We formalize what a design-based simulation holding \mathbf{y} and Ω fixed would recover in this setting, depending on the true treatment effect β and on the presence or absence of spatial correlation in the

³See Goldsmith-Pinkham et al. (2020) for an alternative sampling framework for shift-share designs.

⁴They also allow for clusters of shocks. In this case, the assumption is that shocks from different clusters are independent, the number of clusters of shocks goes to infinity, and the size of each cluster of shocks becomes asymptotically negligible.

empirical application used to construct the DGP used in the simulations.

To this end, consider a simpler version of the shift-share design setting from Section 3.1 in which observations $i = 1, \dots, N$ are partitioned into equally-sized groups $\Lambda_1, \dots, \Lambda_F$, with $w_{if} = 1$ if $i \in \Lambda_f$, and $w_{if} = 0$ otherwise. Assume also that $\mathcal{X}_f \in \{0, 1\}$ and $\sum_{f=1}^F \mathcal{X}_f = F/2$. Potential outcomes are given by $y_i(0) = \beta_0 + \epsilon_i$ and $y_i(1) = \beta + y_i(0)$.⁵ This particular shift-share design setting can be seen as a randomized experiment in which treatment is assigned at the group Λ_f level. In this particular shift-share design setting, the standard error proposed by Adão et al. (2019) would coincide (up to a degrees-of-freedom correction) with standard errors clustered at the group level. Our conclusions in this section can also be extrapolated for DiD designs, which was the setting analyzed by Bertrand et al. (2004).

In this setting, we know that inference based on robust standard errors would be asymptotically valid when $N \rightarrow \infty$ if errors are independent across i . However, it would lead to over-rejection in case errors within partitions are positive correlated. Therefore, it is natural to think that one could run design-based simulations assessing the rejection rates when inference is based on robust standard errors, in order to assess whether spatial correlation leads to relevant size distortions in specific empirical applications. We analyze whether this is actually so.

Consider design-based simulations with random draws of $\tilde{\mathcal{X}}_f \in \{0, 1\}$ such that $\sum_{f=1}^F \tilde{\mathcal{X}}_f = F/2$, while holding \mathbf{y} fixed. More specifically, for each draw of $\tilde{\mathcal{X}}_f \in \{0, 1\}$, we run the regression $y_i = \gamma_0 + \gamma \tilde{x}_i + \tilde{\epsilon}_i$, where $\tilde{x}_i = \sum_{f=1}^F w_{if} \tilde{\mathcal{X}}_f$, yielding $\hat{\gamma}^b$. Then we test the null $\gamma = 0$ using robust standard errors at a significance level α , and calculate the rejection rate in these simulations. The DGP in the simulations sets potential outcomes as $\tilde{y}_i(0) = \tilde{y}_i(1) = y_i$ (which are fixed, given the sampling framework of the simulations) and the distribution for $\tilde{\mathcal{X}}_f$ described above. Therefore, the null hypothesis $H_0 : \gamma = 0$ is true

⁵Given the structure of this shift-share design example, we only need to define the potential outcomes $y_i(x)$ for $x \in \{0, 1\}$.

in this DGP.

Uncertainty in these simulations comes only from realizations of $\tilde{\mathcal{X}}_f$. Let $\mathbb{E}^*[\cdot|\mathbf{y}]$ and $\mathbb{V}^*(\cdot|\mathbf{y})$ denote the expectation and variance operators with respect to this measure, conditional on \mathbf{y} . From Lemma 5 from Barrios et al. (2012), $\mathbb{E}^*[\hat{\gamma}^b|\mathbf{y}] = 0$, so the estimator $\hat{\gamma}^b$ is unbiased. Let $\mathbb{V}_{\text{true}}^* \equiv \mathbb{V}^*(\hat{\gamma}^b|\mathbf{y})$ be the true variance of $\hat{\gamma}^b$ in these design-based simulations. Note that this is a number for a fixed \mathbf{y} , and a random variable depending on the errors ϵ_i when \mathbf{y} is treated as a random variable. Also, let $\mathbb{V}_{\text{robust}}^*$ be the true variance in case treatment were assigned at the individual level in the design-based simulation. This is what the robust standard errors would asymptotically recover in these simulations when $F \rightarrow \infty$.

Therefore, the ratio $\mathbb{V}_{\text{robust}}^*/\mathbb{V}_{\text{true}}^*$ is crucial to understand whether the design-based simulations would indicate or not relevant over-rejections when we assess inference using robust standard errors. Considering this framework with \mathbf{y} fixed, if $\mathbb{V}_{\text{robust}}^*/\mathbb{V}_{\text{true}}^*$ converges to a value smaller than one in a sequence with $F \rightarrow \infty$, this means that the robust variance estimator would tend to underestimate the true variance in the simulations, generating a rejection rate larger than α . In contrast, if $\mathbb{V}_{\text{robust}}^*/\mathbb{V}_{\text{true}}^*$ converges to one in a sequence with $F \rightarrow \infty$, then the robust variance calculated in the simulations would adequately estimate the true variance in the simulations, so we should expect rejection rates in the design-based simulations close to α .

In this setting, we have the following result.

Proposition 3.1. *Consider the shift-share design setting described in this section, and assume the vectors $\{\epsilon_i : i \in \Lambda_f\}$ are iid across f with $\mathbb{E}[\epsilon_i] = 0$, $\mathbb{V}(\epsilon_i) = \sigma^2$, and $\text{cov}(\epsilon_i, \epsilon_s) = \rho$ for $i \neq s$ and $i, s \in \Lambda_f$ for some f . Consider an asymptotic sequence in which $F \rightarrow \infty$ where we maintain that each group Λ_f has exactly m observations (so $N = m \times F$) and $\sum_{f=1}^F \mathcal{X}_f = F/2$. Then*

$$\frac{\mathbb{V}_{\text{robust}}^*}{\mathbb{V}_{\text{true}}^*} \xrightarrow{\text{a.s.}} \frac{\beta^2 + 4\sigma^2}{m\beta^2 + 4\sigma^2 + 4(m-1)\rho}. \quad (2)$$

Proof. See Appendix A.1. □

First, consider a setting with no spatial correlation, so $\rho = 0$. This is a setting in which robust standard errors would be asymptotically valid when $F \rightarrow \infty$. However, Proposition 3.1 shows that, with probability one, $\mathbb{V}_{\text{robust}}^*/\mathbb{V}_{\text{true}}^* \rightarrow k < 1$, whenever the true DGP exhibits a true treatment effect ($\beta \neq 0$) and $m > 1$. Therefore, the design-based assessment would tend to be larger than α , (incorrectly) suggesting that robust standard errors are invalid due to spatial correlation. The intuition is that the true treatment effect β is confounded with spatial correlation that affects the $m > 1$ units within the same partition in a similar way in the DGP used in the simulations. The main problem is that the DGP used in the simulations would differ from the true DGP in a way that is relevant in determining the properties of a specific inference method.

Consider now a setting in which we should expect $\beta = 0$. In this case, with probability one, $\mathbb{V}_{\text{robust}}^*/\mathbb{V}_{\text{true}}^* \rightarrow 1$ when $\rho = 0$. Therefore, if we are in a setting with no spatial correlation (and F is large), rejection rates in this design-based simulation would be close to α , (correctly) suggesting that robust standard errors would be asymptotically valid. In contrast, if we are in a setting with $\rho > 0$, then the rejection rates in the design-based simulations would be larger than α , (correctly) suggesting that robust standard errors are invalid due to spatial correlation. Therefore, even though these simulations hold \mathbf{y} fixed and consider only covariates as stochastic, this formalization also clarifies that, considering a setting with no treatment effect ($\beta = 0$), these simulations are informative about potential problems in the errors, such as spatial correlation. A direct consequence is that, if we want to assess the prevalence of over-rejection due to spatial correlation in a specific setting, then one possibility would be to construct simulations based on a dataset in which we expect the true treatment effect to be zero. If we are analyzing a specific shift-share design empirical application, then one alternative would be to consider simulations using pre-treatment outcomes, so that we should expect similar patterns in terms of spatial correlation of the

potential outcomes, but no treatment effect.

In case pre-treatment data is not available, another alternative to assess the relevance of spatial correlation when $\beta \neq 0$ is to consider ϵ -fixed (rather than \mathbf{y} -fixed) design-based simulations. This is how Borusyak et al. (2021) construct their simulations in their Appendix A.11. In this case, we consider a DGP in which we fix potential outcomes as $\dot{y}_i(0) = \dot{y}_i(1) = y_i - \hat{\beta}x_i$. If potential outcomes in the true model are given by $y_i(x) = y_i + \beta x$ and $\hat{\beta}$ converges almost surely to β when $F \rightarrow \infty$, then we would have simulations with a structure for the potential outcomes that is more similar to the true structure in the application.⁶ Therefore, the ϵ -fixed design-based simulations are informative about the presence of spatial correlation (when $F \rightarrow \infty$), even when we have a true treatment effect $\beta \neq 0$. We formalize this result in Appendix A.1. Interestingly, if treatment effects are heterogeneous or non-linear, then treatment effects would still generate spatially correlated errors in the design-based DGP, even after subtracting $\hat{\beta}x_i$ to construct the potential outcomes for the simulations. Therefore, these simulations would still be informative about problems with robust standard errors in shift-share design regressions due to heterogeneous or non-linear treatment effects.

Remark 2. *The results in this section analyze the properties of design-based simulations as $F \rightarrow \infty$. However, such simulations can also be informative in settings in which F is not large enough for asymptotic approximations to be accurate. For example, if the standard errors proposed by Adão et al. (2019) or Borusyak et al. (2021) (which allow for spatial correlation) underestimate the true variability when the number of sectors is small, design-based simulations may shed light on the magnitude of this distortion. Importantly, when analyzing the finite- F properties of such standard errors, the issue described in Proposition 3.1 is not relevant, since these procedures are valid even in the presence of spatial corre-*

⁶In the stylized setting considered in this setting, the shift-share/OLS estimator $\hat{\beta}$ converges almost surely to β as $F \rightarrow \infty$, even allowing for within-group error correlation. Our argument, however, applies to any estimator $\hat{\beta}$ satisfying $\hat{\beta} \xrightarrow{a.s.} \beta$ under the asymptotic sequence considered, and we therefore maintain this as a high-level assumption.

lation. In this case, the fact that design-based simulations holding \mathbf{y} fixed may artificially induce spatial correlation does not generate an additional problem.

Remark 3. *An additional difficulty in constructing design-based simulations in shift-share settings is that the true distribution of the shocks is generally unknown. This provides a further reason why the DGP considered in such simulations may differ from the true DGP. In Section 5, following Adão et al. (2019), we consider simulations in which shocks are normally distributed with mean zero and homogeneous variance.*

4 Simulations

Appendix A.2 presents simulations illustrating the use of design-based simulations to detect spatial correlation. We consider DGPs that follow the structure of the shift-share design setting analyzed in Section 3.2. The simulations confirm the novel insights presented in Section 3.2: (i) that \mathbf{y} -fixed design-based simulations may incorrectly indicate spatial correlation when the true treatment effect is different from zero; (ii) that ϵ -fixed design-based simulations circumvent this problem; (iii) that \mathbf{y} -fixed design-based simulations can be informative about spatial correlation when $\beta = 0$ (for example, when simulations are based on a placebo specification); and (iv) that ϵ -fixed design-based simulations are informative about inference problems when treatment effects are heterogeneous.

Interestingly, these simulations also highlight an additional insight about the use of design-based simulations. While testing significance in a pre-treatment outcome specification can be informative not only about the possibility of pre-trends but also about spatial correlation (Ferman, 2023), design-based simulations based on pre-treatment outcomes can be even more informative about spatial correlation problems. The intuition is the following. Consider the stylized model from Section 3.2, and assume there are group-level iid shocks that take values $-\omega$ or $+\omega$ with equal probabilities. Let τ_1 (τ_0) denote the proportion of positive shocks among treated (control) groups. Ignoring idiosyncratic shocks, the

pre-treatment outcome regression rejects the null when $|\tau_1 - \tau_0|$ is sufficiently large, as this generates a large point estimate. Thus, rejection requires not only variability in the signs of the shocks, but also an unbalanced allocation of those shocks between treated and control groups. In contrast, design-based simulations analyze rejection rates across all possible treatment assignments rather than only the realized one. As a result, the simulations can flag spatial correlation problems whenever there is sufficient variation in the shocks—so that some treatment assignments would generate large values of $|\tau_1 - \tau_0|$ —even if $|\tau_1 - \tau_0|$ is small for the realized treatment assignment.

5 Empirical illustrations

We illustrate the use of design-based simulations in three shift-share design empirical applications, based on Autor et al. (2013), Dix-Carneiro et al. (2018), and Acemoglu and Restrepo (2020).

5.1 Analyzing distortions due to spatial correlation

We consider first the use design-based simulations to assess the performance of cluster-robust standard errors in these applications. We know that cluster-robust standard errors might be problematic in this setting if (i) there is spatial correlation in the errors (beyond the clusters), and/or (ii) there are few clusters. Ferman (2019) show that, in the absence of spatial correlation, asymptotic approximations for cluster-robust standard errors are relatively less reliable for the weighted OLS specifications in these applications. Since the focus in this section is to understand how different design-based simulations may be used to detect spatial-correlation problems, we therefore focus on the unweighted specifications. We emphasize, though, that those simulations can potentially be used to detect both of these problems.⁷

⁷In order to distinguish between these two problems, one could also run simulations with both errors and shocks stochastic. In this case, we would consider a DGP in which errors are independent, so these

We consider first design-based simulations with \mathbf{y} fixed and stochastic shocks. We find large rejection rates in columns 1, 3 and 5 of Table 1, ranging from 34% to 70%. However, as discussed in Section 3.2, a true treatment effect of x_i may be confounded with spatially-correlated errors in these simulations. Therefore, we could find large rejection rates in these simulations, even when errors are *not* spatially correlated.

We consider the two alternatives discussed in Section 3.2 to assess whether spatial correlation is a relevant concern for cluster-robust standard errors in these applications. All results are presented in Table 1. For the application in Autor et al. (2013), our results reinforce the conclusions of Adão et al. (2019) that spatial correlation leads to substantial over-rejection in this setting. At the same time, the over-rejection we find with these alternative design-based simulations is slightly less severe than that obtained with \mathbf{y} -fixed design-based simulations. This is consistent with the theoretical results presented in Section 3.2, where we show that \mathbf{y} -fixed design-based simulations tend to overstate the magnitude of spatial correlation when there is a true treatment effect.

For Acemoglu and Restrepo (2020), the ϵ -fixed design-based simulations remains large, but the design-based simulations using a placebo outcome is close to 5%. This provides evidence that inference based on cluster-robust standard errors might be reasonable for testing a sharp null of no effect whatsoever, but that we may have relevant heterogeneous treatment effects. As we discuss in Appendix A.3, the simulations using the pre-treatment outcome would have a relatively high probability of flagging problems due to spatial correlation in this application.

Finally, for Dix-Carneiro et al. (2018), both alternative simulations lead to rejection rates smaller than 5%, providing some indication that spatial correlation is not a problem in this application. An important caveat, however, is that those simulations would have a relatively lower probability of flagging a problem in case there is relevant spatial correlation in this application (details in Appendix A.3). An alternative in cases like that may be to

simulations would be informative about the first problem, but not about the second one.

run simulations for a number of pre-treatment outcomes, if available.

5.2 Assessing the reliability of asymptotic approximations

We can also use design-based simulations to assess whether the new inference methods proposed for shift-share designs provide good asymptotic approximations in these settings, given the structure of shares. We find evidence that these inference methods work well in Autor et al. (2013). However, for the other two applications the design-based simulations suggest that these inference methods can lead to large distortions, with rejection rates up to 57% (Table 1, Panel C). This is consistent with these applications having a smaller number of sectors (details in Table 1). Note that it is not a problem to consider \mathbf{y} -fixed design-based simulations in this case, because we are evaluating inference methods that allow for spatial correlation. Therefore, even if a true treatment effect is confounded with spatial correlation in the simulations, this would not be a problem in this case.

5.3 Choosing among alternative inference methods

The results in this section illustrate that it is not trivial to determine which inference methods are more reliable in specific shift-share design applications, and that design-based simulations may be used by applied researchers to inform on that.

If we have evidence that the methods from Adão et al. (2019)/Borusyak et al. (2021) provide accurate asymptotic approximations in a given application, then they should be preferred, as they impose fewer restrictions on the spatial correlation. Therefore, our recommendation is to start with design-based simulations to assess whether inference based on their methods performs well in the application at hand, as we illustrate in Section 5.2. This is the case for the application from Autor et al. (2013).

In case the design-based simulations suggest these new inference methods are unreliable, then the next step should be to use one of the alternative design-based simulations

we propose (design-based simulations on a placebo outcome and/or ϵ -fixed design-based simulations) to evaluate whether inference based on cluster-robust standard errors would be reliable. These design-based simulations would be informative about two potential problems with cluster-robust standard errors in this setting: (i) in case the number of clusters is not large enough, and (ii) in case it is unreasonable to assume that there is no relevant spatial correlation. In our empirical illustrations, we find evidence that inference based on cluster-robust standard errors is relatively more reliable than inference based on these new methods for the applications from Acemoglu and Restrepo (2020) (for testing a sharp null), and from Dix-Carneiro et al. (2018) (with the caveat that the design-based simulations have lower probabilities of detecting problems in this application).

The *placebo* specifications in these two applications provide further evidence on the conclusion that, in these applications, cluster-robust standard errors are relatively more reliable: in both cases, we would reject the null for their *placebo* specifications if we consider Adão et al. (2019) standard errors, while we do not reject these nulls if we use cluster-robust standard errors (Appendix Table A.2, columns 4 and 6). Importantly, if applied researchers consider standard (fixed- y) design-based simulations resampling shocks in these last two applications (instead of the alternatives we propose), they might incorrectly conclude that cluster-robust standard errors are less reliable than the new inference methods in these two applications.

In case we have evidence that none of these methods are reliable, then one would have to consider other alternatives. For example, Borusyak and Hull (2020) and Alvarez et al. (2022) consider the use of randomization inference tests for shift-share designs, and show conditions in which these tests are exact in finite samples even when we allow for unrestricted spatial correlation. However, these tests rely on relatively strong assumptions on the shock assignment mechanism (such as correct specification of the distribution of shocks or exchangeability) for this finite-sample validity. Applied researcher would then have to analyze whether those are reasonable assumptions in their settings.

6 Conclusion

Design-based simulations are widely used in both methodological and applied work to study the finite-sample properties of inference procedures and to evaluate their performance in specific empirical applications. This paper shows that the interpretation of such simulations requires care. Because they construct a DGP by holding realized outcomes fixed, design-based simulations may fail to replicate key features of the true DGP—particularly when treatment effects are present or heterogeneous. In shift-share designs, we show that standard y -fixed simulations can confound treatment effects with spatial correlation, potentially overstating inference distortions.

At the same time, design-based simulations can be informative when properly constructed. We clarify the conditions under which they reveal meaningful features of the error structure and propose alternative simulation designs that better isolate the relevant sources of distortion. Our empirical illustrations demonstrate that the choice of simulation design can materially affect conclusions about the reliability of competing inference methods.

Overall, the usefulness of design-based simulations depends on how closely the simulated DGP aligns with the true one along dimensions that matter for inference. Careful construction and interpretation are therefore essential.

References

- Abadie, A., S. Athey, G. W. Imbens, and J. M. Wooldridge (2020). Sampling-based versus design-based uncertainty in regression analysis. *Econometrica* 88(1), 265–296.
- Abadie, A., S. Athey, G. W. Imbens, and J. M. Wooldridge (2022, 10). When Should You Adjust Standard Errors for Clustering? *The Quarterly Journal of Economics*. qjac038.
- Acemoglu, D. and P. Restrepo (2020). Robots and jobs: Evidence from US labor markets. *Journal of Political Economy* 128(6), 2188–2244.

- Adão, R., M. Kolesar, and E. Morales (2019, 08). Shift-Share Designs: Theory and Inference. *The Quarterly Journal of Economics* 134(4), 1949–2010.
- Alvarez, L., B. Ferman, and R. Oliveira (2022, June). Randomization Inference Tests for Shift-Share Designs. *arXiv e-prints*, arXiv:2206.00999.
- Autor, D. H., D. Dorn, and G. H. Hanson (2013, October). The china syndrome: Local labor market effects of import competition in the united states. *American Economic Review* 103(6), 2121–68.
- Barrios, T., R. Diamond, G. W. Imbens, and M. Kolesar (2012). Clustering, spatial correlations, and randomization inference. *Journal of the American Statistical Association* 107(498), 578–591.
- Bertrand, M., E. Duflo, and S. Mullainathan (2004). How much should we trust differences-in-differences estimates? *Quarterly Journal of Economics*, 24975.
- Borusyak, K. and P. Hull (2020). Non-Random Exposure to Natural Experiments: Theory and Applications. Technical report.
- Borusyak, K., P. Hull, and X. Jaravel (2021, 06). Quasi-Experimental Shift-Share Research Designs. *The Review of Economic Studies*. rdab030.
- de Chaisemartin, C. and J. Ramirez-Cuellar (2024, January). At what level should one cluster standard errors in paired and small-strata experiments? *American Economic Journal: Applied Economics* 16(1), 193–212.
- Dix-Carneiro, R., R. R. Soares, and G. Ulyssea (2018, October). Economic shocks and crime: Evidence from the brazilian trade liberalization. *American Economic Journal: Applied Economics* 10(4), 158–95.
- Ferman, B. (2019, December). Assessing Inference Methods. *arXiv e-prints*, arXiv:1912.08772.
- Ferman, B. (2023). Inference in difference-in-differences: How much should we trust in independent clusters? *Journal of Applied Econometrics* 38(3), 358–369.
- Fisher, R. (1935). *The design of experiments*. 1935. Edinburgh: Oliver and Boyd.
- Goldsmith-Pinkham, P., I. Sorkin, and H. Swift (2020, August). Bartik instruments: What, when, why, and how. *American Economic Review* 110(8), 2586–2624.
- Neyman, J. (1990). On the application of probability theory to agricultural experiments. essay on principles. section 9. *Statistical Science* 5(4), 465–472. Translated from the original 1923 Polish article.

Table 1: **Design-based Simulations for shift-share designs**

	China shock		Exposure to robots		Trade liberalization	
	Main effects	Placebo	Main effects	Placebo	Main effects	Placebo
	(1)	(2)	(3)	(4)	(5)	(6)
Panel A: \mathbf{y} -fixed design-based simulations for cluster-robust standard errors						
Cluster-robust	0.412	0.237	0.330	0.059	0.313	0.001
Panel B: ϵ -fixed design-based simulations for cluster-robust standard errors						
Cluster-robust	0.317	0.226	0.256	0.049	0.012	0.000
Panel C: \mathbf{y} -fixed design-based simulations for new inference methods						
Adão et al. (2019)	0.076	0.098	0.355	0.221	0.547	0.511
Adão et al. (2019) (null imposed)	0.042	0.041	0.296	0.107	0.220	0.116
# of clusters	48	48	48	48	91	91
# of observations	772	772	722	722	411	411
# of sectors	395	395	19	19	20	20

Notes: this table presents different types of design-based simulations for the shift-share applications analyzed in Section 5. We consider both specifications with the main outcome of interest in the original papers (columns 1, 3, and 5), and in which the outcome variable is a placebo (columns 2, 4, and 6). Panels A and C consider design-based simulations holding \mathbf{y} constant. In Panel A we assess inference based on cluster-robust standard errors with HC3 correction, while in Panel C we assess the new inference methods proposed by Adão et al. (2019) (both the standard version and the version with the null imposed). In Panel B, we consider ϵ -fixed design-based simulations to assess inference based on cluster-robust standard errors with HC3 correction. In all cases, design-based simulations are based on random draws of iid standard normal shocks, where we calculate the rejection rate for a 5%-level test. In column 1, we present results from the specifications considered by Adão et al. (2019) in their Section II, which is based on the application from Autor et al. (2013). In column 2, we present the same results, but using a pre-treatment outcome (variation from 1980 to 1990). In columns 3 and 4 we present the assessments for a specification for the main effects and for a placebo specification from Acemoglu and Restrepo (2020). Finally, in columns 5 and 6 we present a specification for the main effects and a placebo specification from Acemoglu and Restrepo (2020). In all cases, we consider unweighted OLS regressions.

A Appendix

A.1 Proof of Proposition 3.1

Proof. Let $\bar{\epsilon}_f := m^{-1} \sum_{i \in \Lambda_f} \epsilon_i$ and $\bar{\epsilon} := N^{-1} \sum_{i=1}^N \epsilon_i = F^{-1} \sum_{f=1}^F \bar{\epsilon}_f$. Let $\mathcal{T} \subset \{1, \dots, F\}$ denote the set of treated groups in the original data ($\mathcal{X}_f = 1$), with $|\mathcal{T}| = F/2$. Write $s_f := \mathbf{1}\{f \in \mathcal{T}\} - \frac{1}{2} \in \{-\frac{1}{2}, \frac{1}{2}\}$ and $t_i := \mathbf{1}\{i \in \Lambda_f \text{ for some } f \in \mathcal{T}\} - \frac{1}{2} \in \{-\frac{1}{2}, \frac{1}{2}\}$. Note that $\sum_{f=1}^F s_f = 0$, $\sum_{f=1}^F s_f^2 = F/4$, $\sum_{i=1}^N t_i = 0$, and $\sum_{i=1}^N t_i^2 = N/4$.

By Lemma 5 and Lemma 2 of Barrios et al. (2012), we can write

$$\mathbb{V}_{\text{true}}^* = \frac{4}{F(F-2)} \sum_{f=1}^F \left(\beta s_f + (\bar{\epsilon}_f - \bar{\epsilon}) \right)^2, \quad (3)$$

$$\mathbb{V}_{\text{robust}}^* = \frac{4}{N(N-2)} \sum_{i=1}^N \left(\beta t_i + (\epsilon_i - \bar{\epsilon}) \right)^2. \quad (4)$$

Now note that:

$$\frac{1}{F} \sum_{f=1}^F \left(\beta s_f + (\bar{\epsilon}_f - \bar{\epsilon}) \right)^2 = \beta^2 \left(\frac{1}{F} \sum_{f=1}^F s_f^2 \right) + \frac{2\beta}{F} \sum_{f=1}^F s_f (\bar{\epsilon}_f - \bar{\epsilon}) + \frac{1}{F} \sum_{f=1}^F (\bar{\epsilon}_f - \bar{\epsilon})^2.$$

Since $|\mathcal{T}| = F/2$, $\frac{1}{F} \sum s_f^2 = \frac{1}{4}$ exactly. For the cross term,

$$\frac{1}{F} \sum_{f=1}^F s_f (\bar{\epsilon}_f - \bar{\epsilon}) = \frac{1}{2F} \sum_{f \in \mathcal{T}} \bar{\epsilon}_f - \frac{1}{2F} \sum_{f \notin \mathcal{T}} \bar{\epsilon}_f - \bar{\epsilon} \cdot \frac{1}{F} \sum_{f=1}^F s_f = \frac{1}{4} (\bar{\epsilon}_{\mathcal{T}} - \bar{\epsilon}_{\mathcal{T}^c}),$$

where $\bar{\epsilon}_{\mathcal{T}} = (F/2)^{-1} \sum_{f \in \mathcal{T}} \bar{\epsilon}_f$ and similarly for \mathcal{T}^c . Because $\{\bar{\epsilon}_f\}_f$ are i.i.d. with $\mathbb{E}[\bar{\epsilon}_f] = 0$ and $\mathbb{E}[|\bar{\epsilon}_f|] < \infty$, the strong law of large numbers (SLLN) gives $\bar{\epsilon}_{\mathcal{T}} \xrightarrow{a.s.} 0$ and $\bar{\epsilon}_{\mathcal{T}^c} \xrightarrow{a.s.} 0$. For the last term,

$$\frac{1}{F} \sum_{f=1}^F (\bar{\epsilon}_f - \bar{\epsilon})^2 = \frac{1}{F} \sum_{f=1}^F \bar{\epsilon}_f^2 - \bar{\epsilon}^2 \xrightarrow{a.s.} \mathbb{E}[\bar{\epsilon}_f^2] - 0 = \mathbb{V}[\bar{\epsilon}_f] = \frac{\sigma^2 + (m-1)\rho}{m},$$

using the SLLN for the i.i.d. sequence $\{\bar{\epsilon}_f^2\}_f$ and $\bar{\epsilon} \xrightarrow{a.s.} 0$. Hence,

$$\frac{1}{F} \sum_{f=1}^F \left(\beta s_f + (\bar{\epsilon}_f - \bar{\epsilon}) \right)^2 \xrightarrow{a.s.} \frac{\beta^2}{4} + \frac{\sigma^2 + (m-1)\rho}{m}. \quad (5)$$

Analogously, for the unit-level expression,

$$\frac{1}{N} \sum_{i=1}^N \left(\beta t_i + (\epsilon_i - \bar{\epsilon}) \right)^2 = \beta^2 \left(\frac{1}{N} \sum_{i=1}^N t_i^2 \right) + \frac{2\beta}{N} \sum_{i=1}^N t_i (\epsilon_i - \bar{\epsilon}) + \frac{1}{N} \sum_{i=1}^N (\epsilon_i - \bar{\epsilon})^2.$$

Again $\frac{1}{N} \sum t_i^2 = \frac{1}{4}$ exactly. The cross term equals $\frac{1}{4}(\bar{\epsilon}_{\text{tr}} - \bar{\epsilon}_{\text{ct}})$, where $\bar{\epsilon}_{\text{tr}} = (N/2)^{-1} \sum_{i: t_i=1/2} \epsilon_i$ and $\bar{\epsilon}_{\text{ct}} = (N/2)^{-1} \sum_{i: t_i=-1/2} \epsilon_i$; by the SLLN, both converge a.s. to 0. Finally, $\frac{1}{N} \sum_{i=1}^N (\epsilon_i - \bar{\epsilon})^2 = \frac{1}{N} \sum_{i=1}^N \epsilon_i^2 - \bar{\epsilon}^2 \xrightarrow{\text{a.s.}} \sigma^2$. Therefore,

$$\frac{1}{N} \sum_{i=1}^N \left(\beta t_i + (\epsilon_i - \bar{\epsilon}) \right)^2 \xrightarrow{\text{a.s.}} \frac{\beta^2}{4} + \sigma^2. \quad (6)$$

Combining Equations 5 and 6,

$$\frac{\mathbb{V}_{\text{robust}}^*}{\mathbb{V}_{\text{true}}^*} = \frac{F-2}{N-2} \cdot \frac{\frac{1}{N} \sum_{i=1}^N (\beta t_i + (\epsilon_i - \bar{\epsilon}))^2}{\frac{1}{F} \sum_{f=1}^F (\beta s_f + (\bar{\epsilon}_f - \bar{\epsilon}))^2} \xrightarrow{\text{a.s.}} \frac{1}{m} \cdot \frac{\frac{\beta^2}{4} + \sigma^2}{\frac{\beta^2}{4} + \frac{\sigma^2 + (m-1)\rho}{m}} = \frac{\beta^2 + 4\sigma^2}{m\beta^2 + 4\sigma^2 + 4(m-1)\rho}.$$

□

A.2 Properties of the ϵ -fixed design-based simulations

We consider the same shift-share design setting and asymptotic sequence described in Section 3.2. In particular, observations are partitioned into equally-sized groups $\Lambda_1, \dots, \Lambda_F$ with $|\Lambda_f| = m$, and potential outcomes satisfy $y_i(0) = \beta_0 + \epsilon_i$ and $y_i(1) = y_i(0) + \beta$, with the dependence structure described in Proposition 3.1.

We now analyze the ϵ -fixed design-based simulations discussed in Section 3.2. Let $\hat{\beta}$ denote an estimator computed from the original sample, and define the ϵ -fixed outcome

$$\dot{y}_i \equiv y_i - \hat{\beta} x_i.$$

In the simulations, we hold $\dot{y} = (\dot{y}_1, \dots, \dot{y}_N)$ fixed and draw $\{\tilde{X}_f\}_{f=1}^F$ uniformly over $\{0, 1\}^F$ subject to $\sum_{f=1}^F \tilde{X}_f = F/2$. For each draw, we construct $\tilde{x}_i = \tilde{X}_f$ for $i \in \Lambda_f$ and run the regression

$$\dot{y}_i = \gamma_0 + \gamma \tilde{x}_i + \tilde{\epsilon}_i,$$

obtaining $\hat{\gamma}^b$.

Let $\mathbb{E}^{**}[\cdot \mid \dot{y}]$ and $\text{Var}^{**}(\cdot \mid \dot{y})$ denote expectation and variance with respect to the

randomization distribution induced by the draws of $\{\tilde{X}_f\}_{f=1}^F$, conditional on \dot{y} . Let

$$V_{\text{true}}^{**} \equiv \text{Var}^{**}(\hat{\gamma}^b \mid \dot{y})$$

denote the true randomization variance in these simulations, and let V_{robust}^{**} denote the variance if we had individual-level assignment. Again, we want to study how the ratio between V_{robust}^{**} and V_{true}^{**} behaves as a function of the true treatment effect and of the spatial correlation. We state as a high-level assumption that $\hat{\beta} \xrightarrow{a.s.} \beta$ as $F \rightarrow \infty$, as our results are valid whenever we have an estimator satisfying this property. We emphasize that this property is satisfied if we consider the shift-share/OLS estimator in this setting.

Proposition A.1. *Consider the same setting and assumptions as in Proposition 3.1. Assume in addition that $\hat{\beta} \xrightarrow{a.s.} \beta$ as $F \rightarrow \infty$ (equivalently, $N \rightarrow \infty$). Then*

$$\frac{V_{\text{robust}}^{**}}{V_{\text{true}}^{**}} \xrightarrow{a.s.} \frac{\sigma^2}{\sigma^2 + (m-1)\rho},$$

which does not depend on β .

Proof. Write the realized outcome in the original sample as $y_i = \beta_0 + \beta x_i + \epsilon_i$, with $x_i = X_f$ for $i \in \Lambda_f$. Define $\Delta \equiv \beta - \hat{\beta}$, so that the ϵ -fixed outcome can be written as

$$\dot{y}_i = y_i - \hat{\beta} x_i = \beta_0 + \epsilon_i + \Delta x_i.$$

Let $T \subset \{1, \dots, F\}$ denote the set of treated groups in the original data (i.e. $f \in T$ iff $X_f = 1$), so $|T| = F/2$, and define the group-level indicators $s_f \equiv \mathbf{1}\{f \in T\} - 1/2 \in \{-1/2, 1/2\}$ and $t_i \equiv \mathbf{1}\{i \in \Lambda_f \text{ for some } f \in T\} - 1/2 \in \{-1/2, 1/2\}$. Also let $\bar{\epsilon}_f \equiv m^{-1} \sum_{i \in \Lambda_f} \epsilon_i$ and $\bar{\epsilon} \equiv N^{-1} \sum_{i=1}^N \epsilon_i = F^{-1} \sum_{f=1}^F \bar{\epsilon}_f$.

By the same randomization-variance algebra used in Proposition 3.1 (Lemma 5 and Lemma 2 of Barrios et al. (2012) applied to the regression of \dot{y} on \tilde{x}), we can write

$$V_{\text{true}}^{**} = \frac{4}{F(F-2)} \sum_{f=1}^F \left(\Delta s_f + (\bar{\epsilon}_f - \bar{\epsilon}) \right)^2, \quad V_{\text{robust}}^{**} = \frac{4}{N(N-2)} \sum_{i=1}^N \left(\Delta t_i + (\epsilon_i - \bar{\epsilon}) \right)^2. \tag{A.1}$$

(These are exactly the expressions in Proposition 3.1 with β replaced by Δ .)

We analyze the limits of the two quadratic averages in (A.1). First, for the group-level

term,

$$\frac{1}{F} \sum_{f=1}^F \left(\Delta s_f + (\bar{\epsilon}_f - \bar{\epsilon}) \right)^2 = \Delta^2 \left(\frac{1}{F} \sum_{f=1}^F s_f^2 \right) + 2\Delta \left(\frac{1}{F} \sum_{f=1}^F s_f (\bar{\epsilon}_f - \bar{\epsilon}) \right) + \frac{1}{F} \sum_{f=1}^F (\bar{\epsilon}_f - \bar{\epsilon})^2. \quad (\text{A.2})$$

Because $|T| = F/2$, we have $\frac{1}{F} \sum_{f=1}^F s_f^2 = 1/4$ exactly. Moreover, $\{\bar{\epsilon}_f\}_{f=1}^F$ are i.i.d. across f , so by the SLLN, $\bar{\epsilon} \xrightarrow{a.s.} 0$ and

$$\frac{1}{F} \sum_{f=1}^F (\bar{\epsilon}_f - \bar{\epsilon})^2 = \frac{1}{F} \sum_{f=1}^F \bar{\epsilon}_f^2 - \bar{\epsilon}^2 \xrightarrow{a.s.} \mathbb{E}[\bar{\epsilon}_f^2] = \text{Var}(\bar{\epsilon}_f) = \frac{\sigma^2 + (m-1)\rho}{m}. \quad (\text{A.3})$$

For the cross average, note that

$$\frac{1}{F} \sum_{f=1}^F s_f (\bar{\epsilon}_f - \bar{\epsilon}) = \frac{1}{F} \sum_{f=1}^F s_f \bar{\epsilon}_f - \bar{\epsilon} \left(\frac{1}{F} \sum_{f=1}^F s_f \right) = \frac{1}{F} \sum_{f=1}^F s_f \bar{\epsilon}_f,$$

since $\sum_{f=1}^F s_f = 0$. Because $\{s_f \bar{\epsilon}_f\}_{f=1}^F$ are i.i.d. across f , with $\mathbb{E}[s_f \bar{\epsilon}_f] = 0$ and $\mathbb{E}[|s_f \bar{\epsilon}_f|] < \infty$, the SLLN implies

$$\frac{1}{F} \sum_{f=1}^F s_f (\bar{\epsilon}_f - \bar{\epsilon}) \xrightarrow{a.s.} 0. \quad (\text{A.4})$$

Since $\Delta = \beta - \hat{\beta} \xrightarrow{a.s.} 0$ by assumption, the first two terms on the right-hand side of (A.2) converge to zero almost surely, while the last term converges almost surely to $(\sigma^2 + (m-1)\rho)/m$ by (A.3). Therefore,

$$\frac{1}{F} \sum_{f=1}^F \left(\Delta s_f + (\bar{\epsilon}_f - \bar{\epsilon}) \right)^2 \xrightarrow{a.s.} \frac{\sigma^2 + (m-1)\rho}{m}. \quad (\text{A.5})$$

Second, for the unit-level term,

$$\frac{1}{N} \sum_{i=1}^N \left(\Delta t_i + (\epsilon_i - \bar{\epsilon}) \right)^2 = \Delta^2 \left(\frac{1}{N} \sum_{i=1}^N t_i^2 \right) + 2\Delta \left(\frac{1}{N} \sum_{i=1}^N t_i (\epsilon_i - \bar{\epsilon}) \right) + \frac{1}{N} \sum_{i=1}^N (\epsilon_i - \bar{\epsilon})^2. \quad (\text{A.6})$$

Because exactly half the units are in treated groups, $\frac{1}{N} \sum_{i=1}^N t_i^2 = 1/4$ exactly. By the SLLN (or standard arguments under the assumed dependence structure), $\bar{\epsilon} \xrightarrow{a.s.} 0$ and

$$\frac{1}{N} \sum_{i=1}^N (\epsilon_i - \bar{\epsilon})^2 = \frac{1}{N} \sum_{i=1}^N \epsilon_i^2 - \bar{\epsilon}^2 \xrightarrow{a.s.} \mathbb{E}[\epsilon_i^2] = \sigma^2. \quad (\text{A.7})$$

For the cross average, note that

$$\frac{1}{N} \sum_{i=1}^N t_i(\epsilon_i - \bar{\epsilon}) = \frac{1}{N} \sum_{i=1}^N t_i \epsilon_i - \bar{\epsilon} \left(\frac{1}{N} \sum_{i=1}^N t_i \right) = \frac{1}{N} \sum_{i=1}^N t_i \epsilon_i,$$

since $\sum_{i=1}^N t_i = 0$. Moreover,

$$\frac{1}{N} \sum_{i=1}^N t_i \epsilon_i = \frac{1}{F} \sum_{f=1}^F s_f \bar{\epsilon}_f,$$

because $t_i = s_f$ for all $i \in \Lambda_f$ and $\sum_{i \in \Lambda_f} \epsilon_i = m \bar{\epsilon}_f$. By the same argument used above, the SLLN implies

$$\frac{1}{N} \sum_{i=1}^N t_i(\epsilon_i - \bar{\epsilon}) \xrightarrow{a.s.} 0. \quad (\text{A.8})$$

Since $\Delta \xrightarrow{a.s.} 0$, the first two terms on the right-hand side of (A.6) converge to zero almost surely. Thus,

$$\frac{1}{N} \sum_{i=1}^N \left(\Delta t_i + (\epsilon_i - \bar{\epsilon}) \right)^2 \xrightarrow{a.s.} \sigma^2. \quad (\text{A.9})$$

Finally, plug (A.5) and (A.9) into (A.1) and use $N = mF$ and $\frac{F(F-2)}{N(N-2)} \rightarrow 1/m^2$ to obtain

$$\frac{V_{\text{robust}}^{**}}{V_{\text{true}}^{**}} = \frac{F(F-2)}{N(N-2)} \cdot \frac{\frac{1}{N} \sum_{i=1}^N \left(\Delta t_i + (\epsilon_i - \bar{\epsilon}) \right)^2}{\frac{1}{F} \sum_{f=1}^F \left(\Delta s_f + (\bar{\epsilon}_f - \bar{\epsilon}) \right)^2} \xrightarrow{a.s.} \frac{1}{m^2} \cdot \frac{\sigma^2}{\frac{\sigma^2 + (m-1)\rho}{m}} = \frac{\sigma^2}{\sigma^2 + (m-1)\rho}.$$

□

A.2 Simulations

We present simulations that illustrate the use to design-based simulations for assessing whether inference is distorted due to spatial correlation. The simulations are based on the simpler shift-share design setting presented in Section 3.2. Let Y_{is} be the outcome for individual i in state s . We have N states, where half of them receive a treatment T_s . Each state has 10 individuals. We consider simulations in which $Y_{is}(0) = \omega \xi_s + \epsilon_{is}$ and $Y_{is}(1) = \beta + Y_{is}(0)$, where ϵ_{is} is iid $N(0, 1)$ across i and s , and ξ_s is iid $N(0, 1)$ across s . The parameter β reflects the true treatment effect, while ω reflects the relevance of state-level shocks. Except for the last set of simulations, β is a fixed parameter in the simulations (so treatment effect is homogeneous).

The goal is to construct design-based simulations to evaluate whether state-level shocks impose relevant distortions for inference based on robust standard errors. For each realization of the potential outcomes $\{Y_{is}(0), Y_{is}(1)\}$, we conduct \mathbf{y} -fixed and ϵ -fixed simulations based on permutations of (T_1, \dots, T_N) . For each permutation we estimate $\hat{\beta}^p$ and conduct inference using robust standard errors, and then calculate the proportion of times in which we would reject the null. Let $\Gamma_{\mathbf{y}}$ (Γ_{ϵ}) be the rejection rate in this given realization of the potential outcomes when we consider the \mathbf{y} -fixed (ϵ -fixed) simulations. We repeat this procedure 20,000 times, so we can study the distribution of $\Gamma_{\mathbf{y}}$ and Γ_{ϵ} across simulations.

The simulation results are presented in Appendix Table A.1. Column 1 presents the test size when we consider inference based on robust standard errors with a nominal level of 5%.⁸ As expected, this is close to 5% when we consider a DGP with no spatial correlation and no heterogeneous treatment effects. However, we have over-rejection when we have spatial correlation or heterogeneous treatment effects. Column 2 presents the probability that the \mathbf{y} -fixed simulations would suggest a rejection rate greater than 10%, which would suggest that there is relevant spatial correlation in this setting (all results remain similar if we consider alternative thresholds), while column 3 presents the probability that the ϵ -fixed simulations would be greater than 10%.

We summarize the main conclusions:

1. As shown in Panels A, when there is a true treatment effect ($\beta \neq 0$), \mathbf{y} -fixed design-based simulations would be larger than, for example, 0.1 (indicating relevant spatial correlation) with a high probability, even when there is no spatial correlation ($\omega = 0$).
2. As also shown in Panel A, the ϵ -fixed design-based simulations would have a much lower probability of indicating relevant spatial correlation when $\omega = 0$. When the number of states increases, the probability that those simulations would incorrectly indicate spatial correlation problems goes to zero.
3. When there is spatial correlation ($\omega \neq 0$), both assessments would be larger than 0.1 with a high probability, correctly indicating that there are relevant spatial correlation problems. This probability is increasing in the number of states (Panels B and C).
4. These simulations are more informative about spatial correlation problems than checking whether there are significant effects in placebo regressions using pre-treatment outcomes (Panel C). For example, in this setting with $\omega = 0.3$, a placebo regression would be significant at 5% in 14% of the time. In contrast, the \mathbf{y} -fixed design-based

⁸For scenarios in which $\beta = 0.5$, this means the rejection rate when we are testing the null $\beta = 0.5$.

simulations would be greater than 0.1 around 74% (91%) of the time when $N = 20$ ($N = 100$). So we may have settings in which the p-value of a placebo regression would be large (which would not raise a red flag for the applied researcher), but these simulations would correctly indicate that there is a problem with a high probability. We discuss the intuition for this result in Section 4.

5. These simulations would also be able to detect problems in case we have heterogeneous treatment effects at the state level (Panel E). In this panel, we consider simulations in which $Y_{is}(0) = \epsilon_{is}$ (so there is no spatial correlation in the error for the potential outcomes when untreated), but $Y_{is}(1) = 0.4\xi_s + Y_{is}(0)$, with $\xi_s \sim N(0, 1)$. Therefore, the superpopulation ATE is still zero, but we have heterogeneous treatment effects for different states.

A.3 Probability of flagging spatial correlation

In Section 5, we discuss the use of design-based simulations to detect spatial correlation in a series of shift-share design applications. Here we consider the probability that those simulations would correctly flag spatial correlation problems in case they are actually present.

We consider the following exercise. Let $w_{if} \geq 0$ be the shares of a given application. We construct an outcome vector given by $Y_i^* = Z_i + \gamma \sum_{f=1}^F w_{if} \mathcal{X}_f^*$, where $Z_i \sim N(0, 1)$, while $\mathcal{X}_f^* \sim N(0, 1)$ are random shocks that will not be the shocks considered by the applied researcher to construct the shift-share variable. We can think of \mathcal{X}_f^* as unobserved variables in the error term that might be spatially correlated. Since those unobservables have the same structure of shares as the real shocks that the applied researcher observes, this spatially correlated shocks may generate relevant over-rejection for inference based on cluster-robust standard errors cluster-robust standard errors cluster-robust standard errors, as discussed by Adão et al. (2019). Note that spatial correlation will be stronger if $|\gamma|$ is larger.

We consider then that the applied researcher runs a shift-share regression using the shift-share variable $X_i = \sum_{f=1}^F w_{if} \mathcal{X}_f$ (where $\mathcal{X}_f \sim N(0, 1)$ are the shocks that she observes), and Y_i^* as the outcome variable. Again, all of those $N(0, 1)$ variables are iid. Since X_i and Y_i^* are independent, the expected value of the shift-share estimator in this DGP is zero.

We consider simulations of this model with the structure of the three applications considered in Section 5. For each realization of these random variables (that generates Y_i^* and X_i), we (i) estimate the shift-share regression, and test the null using cluster-robust

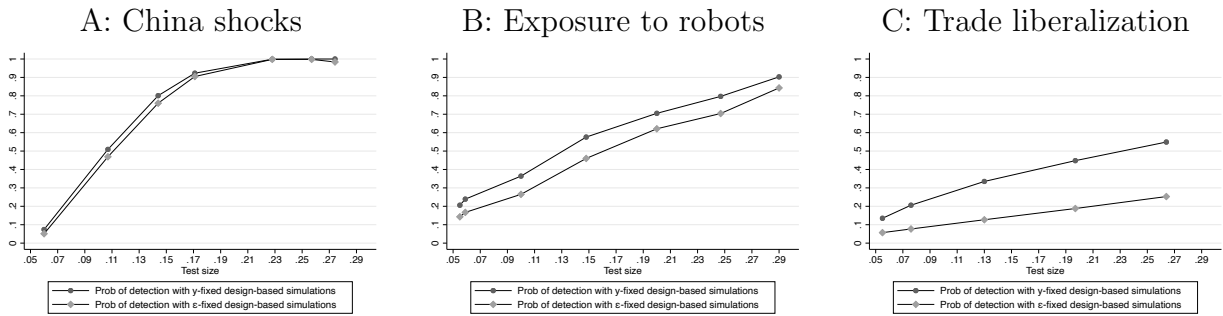
standard errors, and (ii) calculate the rejection rates in \mathbf{y} -fixed and ϵ -fixed design-based simulations. We do that for a number of different values for γ .

For each γ , we also calculate the test size. For all empirical applications, this is close to 5% when $\gamma = 0$ (because there is no spatial correlation in this case). However, when γ increases, then we start to have over-rejection. As a result from these simulations, varying γ , we have information on the true size of the test, and on the proportion of times in which the design-based simulations would flag spatial correlation problems (which we define as having a rejection rate greater than 0.1 in the design-based simulations). We plot in Appendix Figure A.1 the probability of flagging a problem as a function of the test size (which, in turn, is a function of γ).

For the application from Autor et al. (2013), these simulations would have a large probability of detecting problems, when there is spatial correlation. For example, if the spatial correlation is such that the test size using cluster-robust standard errors is 17%, there would be a 90% chance that the design-based simulations would flag spatial correlation problems. For the application from Acemoglu and Restrepo (2020), the probability of detecting problems is a bit lower. For example, if the spatial correlation is such that the test size is around 15%, there would be a 60% probability of flagging spatial correlation problems. If the spatial correlation is stronger, then the probability of detecting problems would be larger. Finally, we note that the probability of detecting problems is much smaller for the application from Dix-Carneiro et al. (2018). When the test size is around 15%, we would only have a 35% probability that these design-based simulations would suggest that there are relevant spatial correlation problems.

In case the design-based simulations do not detect problems due to spatial correlation, we recommend that applied researchers consider this kind of simulations. This way, they can evaluate whether these simulations would have a high probability of detecting problems when there are meaningful spatial correlation problems. Also, we note that we can make these simulations more informative about spatial correlation problems in case we can combine information from multiple placebo outcomes.

Figure A.1: Probability of detecting spatial correlation problems



Notes: these figures present the results from the simulations described in Section A.3. Each point in the graphs represent one choice of γ , which determines the strength of the spatial correlation in the DGP used in the simulations. For that γ , we plot the implied rejection rate for inference using cluster-robust standard errors (which is increasing in $|\gamma|$), and the probabilities that the rejection rates in the design-based simulations are greater than 0.1. We consider the application from Autor et al. (2013) in Figure A, the one from Acemoglu and Restrepo (2020) in Figure B, and from Dix-Carneiro et al. (2018) in Figure C.

Table A.1: **Design-based simulations**

	Test size (1)	$\Pr(\Gamma_{\mathbf{y}} > 0.1)$ (2)	$\Pr(\Gamma_{\epsilon} > 0.1)$ (3)
Panel A: positive treatment effect ($\beta = 0.5$), but no spatial correlation ($\omega = 0$)			
$N = 20$	0.051	0.632	0.091
$N = 100$	0.049	0.715	0.008
Panel B: positive treatment effect ($\beta = 0.5$), and spatial correlation ($\omega = 0.3$)			
$N = 20$	0.140	0.927	0.688
$N = 100$	0.138	0.998	0.902
Panel C: no treatment effect ($\beta = 0$), and spatial correlation ($\omega = 0.3$)			
$N = 20$	0.140	0.743	0.689
$N = 100$	0.138	0.913	0.902
Panel D: no treatment effect ($\beta = 0$), and no spatial correlation ($\omega = 0$)			
$N = 20$	0.051	0.114	0.091
$N = 100$	0.049	0.009	0.008
Panel E: heterogeneous treatment effects			
$N = 20$	0.129	0.672	0.615
$N = 100$	0.130	0.840	0.826

Notes: this table presents the results from the simulations discussed in Section A.2. Column 1 presents test size for inference based on robust standard errors, with a nominal level of 5%. Column 2 (column 3) presents the probability that the \mathbf{y} -fixed design-based simulations (ϵ -fixed design-based simulations) are greater than 0.1. This would flag that inference based on robust standard errors might be problematic due to spatial correlation (all results remain similar if we consider alternative thresholds). We run 20,000 simulations (draws of the original data) for each scenario, and for each draw $\Gamma_{\mathbf{y}}$ and Γ_{ϵ} are constructed using 500 permutations.

Table A.2: **Shift-share designs: point estimates and standard errors**

	China shock		Exposure to robots		Trade liberalization	
	Main effects	Placebo	Main effects	Placebo	Main effects	Placebo
	(1)	(2)	(3)	(4)	(5)	(6)
Estimate	-0.504	-0.110	-0.516	-0.217	-1.976	0.727
CRVE						
Standard error	0.103	0.048	0.118	0.151	0.822	1.096
p-value	0.000	0.023	0.000	0.152	0.016	0.508
CRVE - HC3						
Standard error	0.116	0.052	0.150	0.226	0.839	1.147
p-value	0.000	0.034	0.001	0.338	0.018	0.526
Adão et al. (2019)						
Standard error	0.138	0.036	0.053	0.070	0.311	0.227
p-value	0.000	0.003	0.000	0.002	0.000	0.001
Adão et al. (2019) (null imposed)						
Standard error	0.208	0.048	0.115	0.342	0.545	0.442
p-value	0.016	0.022	0.000	0.525	0.000	0.100
# of clusters	48	48	48	48	91	91
# of observations	772	772	722	722	411	411
# of sectors	395	395	19	19	20	20

Notes: this table presents the estimates, standard errors, and p-values when we consider inference based on cluster-robust standard errors (CRVE), cluster-robust standard errors with HC3 correction (CRVE - HC3), and the procedure proposed by Adão et al. (2019) (without and with the null imposed). Columns 1 and 2 refer to the application from Autor et al. (2013). We consider the specification that Adão et al. (2019) used in their Table I. Column 1 uses estimates for the main effects, while column 2 uses a placebo specification (considering variations in the outcome variable from 1980 to 1990). Columns 3 and 4 refer to the application from Acemoglu and Restrepo (2020). Column 3 uses the specification from column 6 in their Table 2, while column 4 uses the specification from column 4 in their Table 4. Columns 5 and 6 refer to the application from Dix-Carneiro et al. (2018). Column 5 uses the specification from column 1 in their Table 2, while column 6 uses the specification from column 1 in their Table 4.